RSC Advances

PAPER

View Article Online
View Journal | View Issue

Cite this: *RSC Adv.*, 2017, **7**, 14528

Strategies for fast ion transport in electrochemical capacitor electrolytes from diffusion coefficients, ionic conductivity, viscosity, density and interaction energies based on HSAB theory†

Morihiro Saito,*[a] Satoru Kawaharasaki,[a] Kensuke Ito,[a] Shinya Yamada,[a] Kikuko Hayamizu[b] and Shiro Seki[c]

To elucidate factors affecting ion transport in capacitor electrolytes, five propylene carbonate (PC) electrolytes were prepared, each of which includes a salt ($(C_2H_5)_4NBF_4$, $(C_2H_5)_4NPF_6$, $(C_2H_5)_4NSO_3CF_3$, $(C_2H_5)_3CH_3NBF_4$ and $LiBF_4$). In addition to conventional bulk parameters such as ionic conductivity (σ), viscosity (η) and density (ρ), self-diffusion coefficients (D) of the cation, anion and PC were measured by pulsed-gradient spin-echo (PGSE) NMR. Interaction energies (ΔE) were calculated by density function theory calculations based on Hard and Soft Acids and Bases (HSAB) theory for cation–anion (salt dissociation) and solvent–cation/anion (solvation). ΔE values are related to the salt dissociation and solvation, which affect ion diffusion radii formed by solvation and/or ion pairs. The calculated solvation ΔE values were small (around 0.30 eV) and salt dissociation energies were also small. For comparison, the ΔE value for PC–Li^+ interaction was larger than that for ammonium cations, because of strong Li^+ Lewis acidity. Ammonium salts are highly dissociated and each ion forms a weakly solvated structure, which is quite different from Li^+ electrolytes. Weak solvation for the cation and anion in the ammonium salts are important in enhancing fast ion transfer and electrode reactions in capacitor devices.

Received 11th January 2017
Accepted 24th February 2017

DOI: 10.1039/c7ra00455a

rsc.li/rsc-advances

Introduction

Electric double-layer capacitors (EDLCs) have received increasing attention for power supply systems, not only for small electric devices, such as smart phones and tablet computers, but also in electric vehicles. The advantages of EDLCs include their high-rate capability and semi-permanent long cycle life, which are derived from their fast charge/discharge mechanism owing to the electric double layer of activated carbon (AC) electrodes that do not undergo faradaic reactions (electrochemical redox reactions).[1–6] The cell performance of EDLCs therefore depends significantly on the electrolyte properties, *i.e.*, the ion transport rate and electrochemical stability of the electrolytes. However, EDLC systems provide relatively small electrical capacitance because only the surfaces of the AC positive (PE) and negative (NE) electrodes are used. In recent years, due to the requirements for increased energy density of EDLCs, lithium ion capacitors (LICs), including faradaic-reaction NEs using graphite or hard carbon, have been intensively developed to overcome the low energy density limitation of EDLCs.[6–11] Many researchers have evaluated the viscosity η, ionic conductivity σ and density ρ of electrolyte solutions, together with their electrochemical stability (potential window).[12–15] Dielectric constants of solvents and degree of dissociation α of salts were also investigated to evaluate the solubility and dissociation of salts in these electrolytes.[15,16] These physical parameters are important and useful for the design of suitable electrolytes for EDLCs and LICs. Physical parameters provide understanding of the macroscopic behaviours of electrolytes; however, to design new electrolyte systems for next-generation capacitors, more direct microscopic information is necessary, such as individual transport rates of ions and solvent, and their relationships with interaction energies between the components of the capacitor electrolytes.

This study targeted four electrolytes used in EDLCs and one electrolyte comprising a lithium salt used for LICs. Fig. 1 shows the chemical structures of cations and anions in the salts used in this study. We measured individual self-diffusion coefficients D of the ions and solvent in these capacitor electrolytes by pulsed gradient spin-echo nuclear magnetic resonance (PGSE-NMR), together with conventional physical properties, *i.e.*,

[a]*Department of Applied Chemistry, Faculty of Engineering, Tokyo University of Agriculture & Technology, 2-24-16 Naka-cho, Koganei-shi, Tokyo 184-8588, Japan. E-mail: mosaito@cc.tuat.ac.jp; Fax: +81-42-388-7095; Tel: +81-42-388-7095*

[b]*Institute of Applied Physics, University of Tsukuba, 1-1-1 Tennoudai, Tsukuba, Ibaraki 305-8573, Japan*

[c]*Materials Science Research Laboratory, Central Research Institute of Electric Power Industry (CRIEPI), 2-6-1 Nagasaka, Yokosuka-shi, Kanagawa 240-0196, Japan*

† Electronic supplementary information (ESI) available. See DOI: 10.1039/c7ra00455a

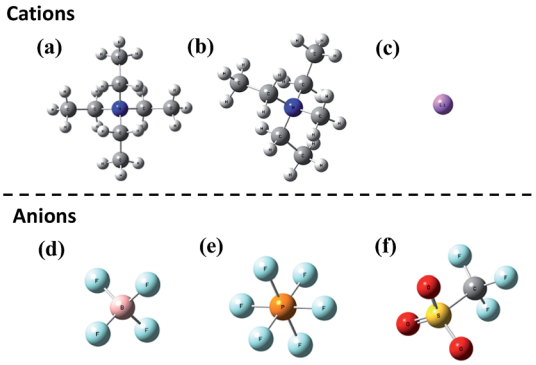

Fig. 1 Chemical structures of the cations and anions used in this study, as optimized by DFT calculation using a basis set of B3LYP/6-311+G**//HF/3-21G. (a) $(C_2H_5)_4N$ (TEA^+), (b) $(C_2H_5)_3CH_3N$ ($TEMA^+$), (c) Li^+, (d) BF_4^-, (e) PF_6^- and (f) CF_3SO_3 (OTf^-).

ionic conductivity σ, viscosity η and density d, of the electrolytes, and discuss these with respect to ion transport behaviour. The relationships between the D values and the other conventional properties are analysed and discussed from the viewpoint of mobility and number of carrier ions in the electrolytes. To elucidate the relationship between the interactions between the chemical species and ion transport behaviour in the electrolytes, we also estimated the interaction energies between the cation–anion, propylene carbonate (PC)–cation and PC–anion by density function theory (DFT) calculation based on the Hard and Soft Acids and Bases (HSAB) theory[17–19] for each electrolyte.

Experimental

We used five different 1.0 M (mol L^{-1}) electrolyte solutions of ammonium salts, *i.e.*, $(C_2H_5)_4NBF_4$ ($TEABF_4$, Kishida Chemical Co., Ltd.), $(C_2H_5)_4NPF_6$ ($TEAPF_6$, Aldrich), $(C_2H_5)_4NSO_3CF_3$ (TEAOTf, Wako Pure Chemicals), $(C_2H_5)_3CH_3NBF_4$ ($TEMABF_4$, Tokyo Chemical Industry Co., Ltd.) and $LiBF_4$ (Kishida Chemical Co., Ltd.) in propylene carbonate (PC, battery grade, Wako Pure Chemicals). Prepared samples were stored in an Ar-filled dry box (VAC, NEXUS II).

Ionic conductivity σ of the electrolytes was measured in hermetically sealed cells [stainless steel (SUS)/electrolyte/SUS] and determined by complex impedance using an AC impedance analyser (Bio-Logic VSP, 200 kHz to 50 mHz; applied voltage: 10 mV) in the temperature range of 283 to 353 K. The electrolytes were thermally equilibrated at each temperature for at least 90 min prior to the measurement.

The self-diffusion coefficients of the cation (^1H or ^7Li), anion (^{19}F) and solvent PC (^1H) in the electrolytes were measured by PGSE-NMR using a JEOL tunable pulsed-field gradient (PFG) probe and an amplifier with a 6.4 T wide-bore superconducting magnet (^1H resonance: 270 MHz) between 353 and 253 K.[20–23] Each sample was prepared in an NMR microtube (BMS-005J, Shigemi, Tokyo) to a height less than 5 mm to prevent convection effects. The calibration of the PFG was made by H_2O (^1H resonance) and D_2O (^2H resonance). Measurements were made by setting the PFG strength to 0.84 to 1.3 T m^{-1} for ^1H and ^{19}F and 2.5 T m^{-1} for ^7Li for varying duration times. The PFG interval (Δ) was set between 20 and 50 ms, depending on temperature. The confirmation of the accuracy of the diffusion constant was carried out by obtaining the same value with different Δ's.

Measurements of viscosity η and density ρ were carried out using a Stabinger-type viscometer (SVM3000G2, Anton Paar). The temperature was controlled in the range of 283 to 353 K at 10 K intervals while heating the samples.

The more quantitative cation–anion and PC–cation interactions were investigated by *ab initio* Hartree–Fock (HF) self-consistent field molecular orbital calculation and DFT calculation performed by Gaussian 09 software.[24] The geometries of the cations, anions and PC were optimized by DFT using the B3LYP form for the exchange–correlation function and the 6-311+G** basis set after HF optimization with the 3-21G basis set. From results of the total electron energy of the ions and solvent, the cation–anion, PC–cation and PC–anion interaction energies were estimated by equations based on HSAB theory.[17–19]

Results

Fig. 2 shows the temperature dependences of σ for the 1.0 M PC-based electrolytes with (a) a common cation (TEA^+) and different anions (BF_4^-, PF_6^- and OTf^-) and (b) a common anion (BF_4^-) and different cations (TEA^+, $TEMA^+$ and Li^+). All plots veered slightly towards higher values, but approximately followed an Arrhenius-type plot. For the common cation, the ionic conductivity decreased in order of $TEABF_4$ > $TEAPF_6$ > TEAOTf across the entire temperature range from 283 to 353 K. In contrast, for the common anion (BF_4^-), the ionic conductivity

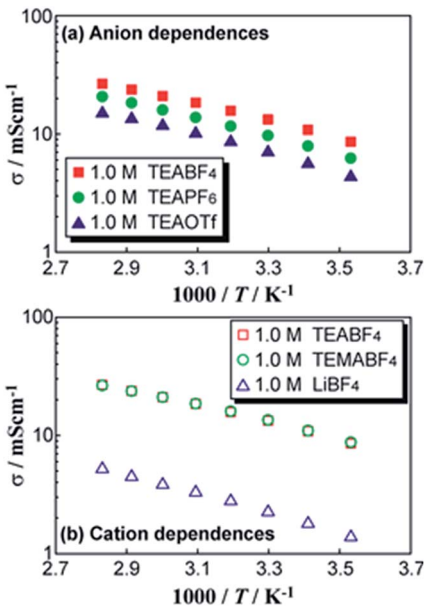

Fig. 2 Comparison of temperature dependences of ionic conductivity σ for 1.0 M PC-based electrolytes with (a) a common cation (TEA^+) and different anions (BF_4^-, PF_6^- and OTf^-) and (b) a common anion (BF_4^-) and different cations (TEA^+, $TEMA^+$, and Li^+). The values for $TEABF_4$ and $TEMABF_4$ almost overlap.

changed in the order $TEMABF_4 \approx TEABF_4 \gg LiBF_4$. The trend in ionic conductivity for the ammonium salt-based electrolytes was in good agreement with those reported by Ue *et al.*, for a salt concentration of 0.65 M at 298 K.[1] The $LiBF_4$-based electrolyte exhibited one order of magnitude lower σ than the ammonium salt-based electrolytes. This difference will be described later.

The ionic conductivity of electrolytes was defined by eqn (1):

$$\sigma = \sum_j q_j \times \mu_j \times n_j \quad (1)$$

where q, μ and n are the charge, mobility and number of carrier ions per specific volume, respectively; the suffix j corresponds to the ammonium cations and anions. Ionic conductivity of electrolytes depends on (i) mobility and (ii) number of carrier ions per specific volume. Here, to consider the mobility μ of each carrier ion, we separately measured the D values of the cation, anion and PC solvent by PGSE-NMR. Typical Arrhenius-type plots for 1.0 M PC-based electrolytes containing $TEABF_4$ and $TEAPF_6$ are shown in Fig. 3. Except at high temperature, the diffusion constants of $TEABF_4$ are larger than those of $TEAPF_6$; within the same electrolyte, $D_{PC} > D_{anion} > D_{TEA}$. Summaries of the data for the other electrolytes are shown in Tables 1 (D) and 2 (η) in ESI.† For a single electrolyte, the order of the D values was PC > anion (BF_4^-, PF_6^-, TfO^-) > cation ($TEMA^+$, TEA^+, Li^+) across the entire temperature range evaluated. The temperature dependences essentially followed Arrhenius-type plots, indicating that the ions are transported by flow of the PC solvents and that the anions move more easily than the cations in these electrolytes. This trend was similar to those reported for electrolyte solutions for lithium ion batteries (LIB).[20] The order of magnitude of D for the four ammonium electrolytes and the lowest D for a 1.0 M $LiBF_4$/PC are in good agreement with the trend for σ. This indicates that σ is significantly influenced by mobility μ of the carrier ions.

From the temperature dependences, the activation energies of D, *i.e.*, E_a, were estimated from the slopes of plots for the electrolyte systems, as shown in Table 1. For all electrolytes, including $LiBF_4$/PC, the E_a values were around 0.20 eV. The E_a values in these capacitor electrolytes were of the same scale as those of LIB electrolytes. This means that all chemical species are transported in a similar way in these electrolytes.

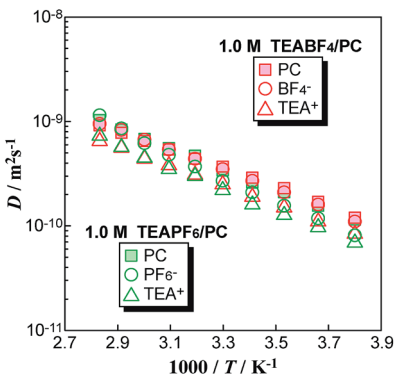

Fig. 3 Typical temperature dependences of self-diffusion coefficients D for 1.0 M PC-based electrolytes containing $TEABF_4$ and $TEAPF_6$.

Table 1 Activation energies E_a from Arrhenius-type plots of D for ions and PC solvents and transference numbers of cations t_{cation} at 303 K for 1.0 M PC-based electrolytes

	D_{PC}	D_{cation}	D_{anion}	
Electrolyte solution	E_a/eV	E_a/eV	E_a/eV	t_{cation}
1.0 M $TEABF_4$/PC	0.18	0.20	0.18	0.42
1.0 M $TEAPF_6$/PC	0.20	0.23	0.21	0.45
1.0 M TEAOTf/PC	0.21	0.22	0.21	0.45
1.0 M $TEMABF_4$/PC	0.23	0.22	0.24	0.43
1.0 M $LiBF_4$/PC	0.22	0.23	0.25	0.42

From the D values of the cations and anions, the apparent transference numbers of the cations were calculated by eqn (2), as follows:

$$t_{cation} = D_{cation}/(D_{cation} + D_{anion}) \quad (2)$$

The results at 303 K are shown in Table 1 (values for each t_{cation} by temperature are summarized in S1†). All t_{cation} values were around 0.40, which is also similar to those reported for LIB electrolytes.[20]

In general, the σ and D values are strongly related to the viscosity of the electrolyte. The D values of electrolyte solutions are known to increase with the decrease in viscosity. Fig. 4 shows the temperature dependences of η^{-1} for 1.0 M PC-based electrolyte solutions in (a) a common TEA^+ cation with three anions and (b) a common BF_4^- anion with three cations. The η^{-1} values for all electrolytes followed the trend of temperature dependences: $TEABF_4$ > $TEAPF_6$ > TEAOTf and $TEMABF_4 \approx TEABF_4 \gg LiBF_4$. Because we used PC as a solvent in all

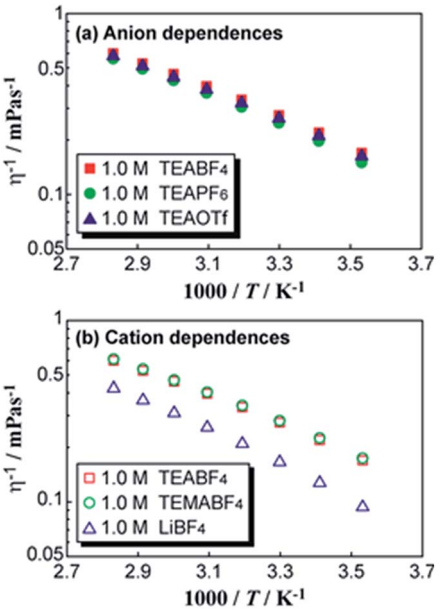

Fig. 4 Temperature dependences for inverse of viscosity η^{-1} values for 1.0 M PC-based electrolytes in (a) a common TEA^+ with different anions and (b) a common BF_4^- with different cations.

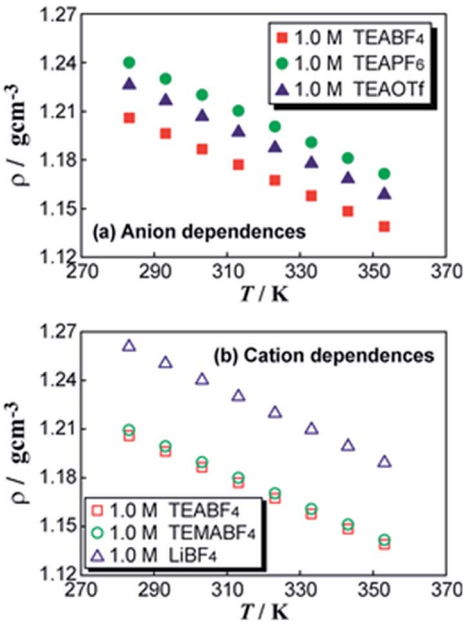

Fig. 5 Comparison of temperature dependence of density ρ for 1.0 M PC-based electrolytes for (a) anions and (b) cations.

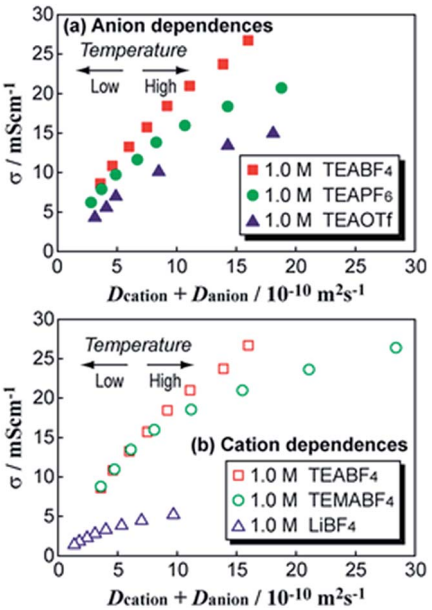

Fig. 6 Plots of ionic conductivity σ against the sum of (D_{cation} + D_{anion}) for (a) common TEA^+ with three different anions and (b) common BF_4^- with three different cations for 1.0 M PC electrolytes.

samples, the dominant effects on the viscosity were induced by the dissolved salt. The η^{-1} values showed good correspondence with σ and D values.

Fig. 5 shows the density ρ of the electrolytes as a function of temperature. The ρ values linearly decreased with increase of temperature: $TEABF_4$ < $TEAPF_6$ < TEAOTf and $TEMABF_4$ ≈ $TEABF_4$ < $LiBF_4$. This is also in good agreement with the trend of the η values. This implies that an electrolyte with smaller ρ exhibits a lower η and higher D owing to the larger space available for the carrier ions to move in the present samples. The observed data for the $LiBF_4$-based electrolyte deviated considerably in σ, η^{-1} and ρ, but not in D values. This means that the interaction in the electrolyte is quite strong for Li^+ and there is a smaller space for the ions and PC solvent to move than that in the ammonium salt-based electrolytes.

Discussion

To observe the effect of mobilities μ of the carrier ions on ionic conductivity σ, the σ values are plotted against the sum of D_{cation} + D_{anion} in Fig. 6 for (a) a common TEA^+ cation with three different anions and (b) a common BF_4^- anion with three different cations. The σ values increased with an increase in (D_{cation} + D_{anion}) for all electrolytes. The cation and anion diffusion constants clearly influence the σ values. In the common TEA^+ systems, the σ values depend on the counter-anions in the order BF_4^- > PF_6^- > OTf^-, although the ion diffusion constants were slightly modulated by the anions. In the common BF_4^- systems, the σ values are similar in the TEMA–BF_4 and TEA–BF_4 electrolytes, but the TEMA–BF_4 electrolyte exhibited larger (D_{cation} + D_{anion}). The $LiBF_4$ electrolyte showed exceptionally smaller σ and (D_{cation} + D_{anion}) values, suggesting different solution structures. The ammonium cations, especially $TEMA^+$, therefore have an advantage from the viewpoint of mobility when compared with Li^+.

As mentioned above, ion transport in capacitor electrolytes is considered to occur *via* a vehicle mechanism. The relationship between D and η can therefore be defined by the Stokes–Einstein equation,[11] as follows:

$$D = kT/c\pi\eta r_{ion} \quad (3)$$

where k is Boltzmann's constant, T is temperature (K), η is viscosity of the electrolyte (Pa s^{-1}), r_{ion} is the Stokes (solvated ion) radius (m) and c is a constant, which ranges between 4 and 6 for slip and stick boundary conditions, respectively.[25] Eqn (3) implies that an electrolyte with lower viscosity exhibits higher D value of the solvent. Fig. 7 shows the self-diffusion coefficients of PC, D_{PC}, plotted against η^{-1} of the electrolytes. For all electrolytes, D_{PC} increased with increase of η^{-1}, according to eqn (3). At high temperatures, deviations from linear plots suggested interactions between PC and the ions.

In eqn (3), c and η are assumed to be the same for the ions and PC, so the r_{ion}/r_{PC} value is simply defined as eqn (4):[22]

$$r_{ion}/r_{PC} = D_{PC}/D_{ion} \quad (4)$$

The r_{ion}/r_{PC} value represents the effective radius of the diffusing ion in the electrolyte because the PGSE-NMR method gives average values of self-diffusion coefficients of the ions and PC. Table 2 shows the relative ion radius relative to PC (r_{ion}/r_{PC}) for the five electrolytes.

Based on their molecular structures, the ionic radii of TEA^+, $TEMA^+$, Li^+, BF_4^-, PF_6^-, OTf^-, and PC were calculated as 0.343, 0.327, 0.076, 0.229, 0.254, 0.270 and 0.276 nm, respectively.[12] In the present study, except for $LiBF_4$, the orders of magnitude of

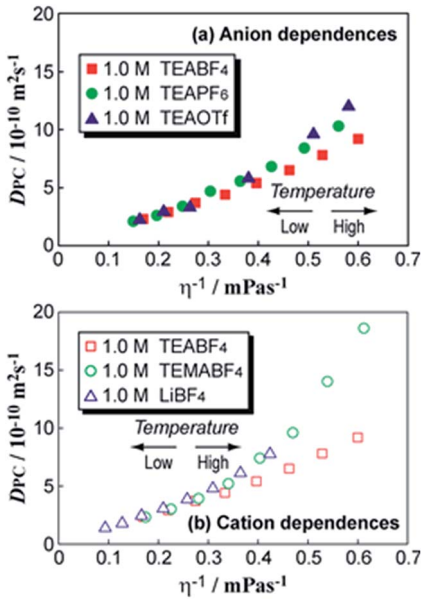

Fig. 7 Plots of solvent self-diffusion coefficients D_{PC} against the inverse of viscosity η^{-1} for 1.0 M PC electrolytes in (a) common TEA^+ with three different anions and (b) common BF_4^- with three different cations.

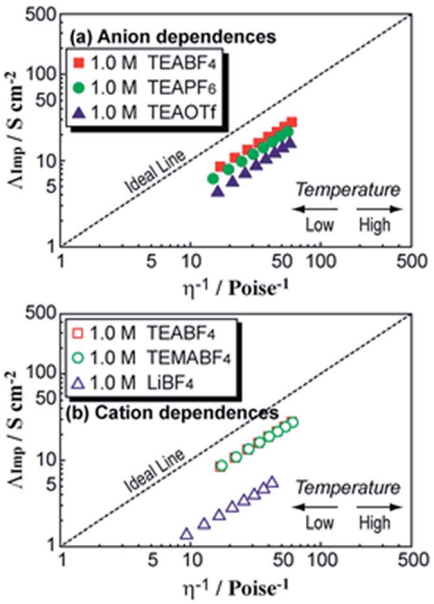

Fig. 8 Walden plots for 1.0 M PC electrolytes for (a) TEA^+ with three different anions and (b) BF_4^- with three different cations.

Table 2 Ionic radius relative to PC (r_{ion}/r_{PC}) in the capacitor electrolytes at 303 K, calculated using eqn (4)

Species	$TEABF_4$	$TEAPF_6$	TEAOTf	$TEMABF_4$	$LiBF_4$
Anion	1.1	1.3	1.2	1.1	1.7
Cation	1.5	1.5	1.5	1.5	2.4

the r_{ion}/r_{PC} values of the cations and anions calculated from the D_{ion}'s agreed relatively well with the estimated values from the van der waals' radii; however, all r_{ion}/r_{PC} values were slightly larger than those from the radii, implying the formation of weak solvation structures and ion pairs between the solvent and/or counterions. In contrast, the r_{ion}/r_{PC} values of Li^+ and BF_4^- in the $LiBF_4$ electrolyte were much larger. This indicates that either Li^+ interacts strongly with PC to form a solvated $Li^+(PC)_x$ species or that BF_4^- contributes to the formation of ion pairs. As a result, Li^+ and BF_4^- in the electrolyte diffuse more slowly than the ions in the TEA and TEMA electrolytes. In addition, the r_{Li}/r_{PC} value of Li^+ was about 2.4, implying that the number of solvated PC molecules with Li^+ was in the range of 2 to 4. In general, it is known that Li^+ is solvated by *ca.* four PC molecules.[26] The r_{Li}/r_{PC} value obtained by our method therefore includes exchange between molecules in the bulk PC and is in good agreement with the assumed value. In the EDLC electrolytes, the values of r_{TEA}/r_{PC} and r_{TEMA}/r_{PC} suggest that the ammonium cations interact weakly with PC and/or the counteranions to form weak solvation structures and ion pairs.

As shown by eqn (1), the ionic conductivity of solution electrolytes is also influenced by the number of carrier ions n per specific volume. To clarify the effect of the n on σ, we conducted analyses using Walden plots and the Nernst–Einstein equation.

Fig. 8 shows the Walden plots for (a) a common TEA^+ cation and three different anions and (b) a common BF_4^- anion and three different cations. Here, ionic conductivity σ was converted to molar conductivity Λ_{imp} using the densities ρ given in Fig. 5. The Walden plots deviated downward from the ideal line. In the common TEA^+ electrolytes (Fig. 8(a)), the deviation became little larger on changing from BF_4^- to PF_6^- to OTf^-, following the anion size. In the common BF_4^- electrolytes (Fig. 8(b)), the plots of TEA^+ and $TEMA^+$ overlapped, but that for the Li electrolyte deviated considerably.

The molar ionic conductivity Λ_{NMR} can be calculated from the self-diffusion coefficients (D_+, D_-) by the Nernst–Einstein equation, as follows:

$$\Lambda_{NMR} = Ne^2(D_+ + D_-)/kT \quad (5)$$

where N is the number of isolated ions per specific volume. Eqn (5) holds for electrolytes in which ions are perfectly dissociated (such as in an infinite diluted solution). From the D_+ and D_- determined by PGSE-NMR measurements, the experimental Λ_{NMR} values were calculated for the five electrolytes. PGSE-NMR data provide the average D values for all ions, including isolated and paired ions. NMR measurements cannot distinguish charged (isolated) ions from paired ions, so the experimental Λ_{NMR} includes whole diffusion species. We have confirmed that at infinite dilution in lithium organic solutions, eqn (5) exactly holds.[21] In practical electrolytes, the calculated experimental Λ_{NMR} is always larger than Λ_{imp} at all temperatures. The apparent degree of ion dissociation, α_{app} in solution electrolytes can be determined from eqn (6):[20–22]

$$\alpha_{app} = \Lambda_{imp}/\Lambda_{NMR}. \quad (6)$$

Fig. 9 shows the temperature dependences of the α_{app} values. At 303 K, the α_{app} is largest for $TEABF_4$, followed by the order $TEABF_4$ > $TEAPF_6$ ≈ $TEMABF_4$ > TEAOTf ≫ $LiBF_4$. Generally, the α_{app} values are insensitive to temperature, except for the $TEAPF_6$ and $TEMABF_4$ electrolytes. At a glance, it is a little strange that the degree of ion dissociation decrease in the higher temperatures for $TEAPF_6$ and $TEMABF_4$. At the present stage, however, we cannot clearly explain the reasons why the α_{app} is insensitive to temperature. More studies are required to interpret the temperature dependent ion–solvent and ion–ion interactions.

The Walden plots and α_{app} values indicate that ion dissociation is higher for TEA^+ and $TEMA^+$ ammonium salts than that for $LiBF_4$. The magnitude of deviation in the Walden plots agrees with the order of ion dissociation α_{app}: $TEABF_4$ > $TEAPF_6$ > TEAOTf and $TEABF_4$ ≈ $TEMABF_4$ ≫ $LiBF_4$. This trend is in good agreement with those estimated from Λ_{imp} and the limiting molar conductivity Λ_0 values reported by Ue *et al.*[16] From the number of carrier ions, this order also agreed well with that of σ. Ionic conductivity of the electrolytes is, therefore also closely related to the concentration of carrier ions.

Mobility and concentration of the carrier ions are strongly related to physical parameters (η, ρ and D) and it is necessary to understand the mutual interactions between cation–anion, PC–cation and PC–anion. Here, we calculated these three interaction energies ΔE using DFT and HSAB calculations.[16–18] When an interaction occurs, for example, between M1 and M2, the change in the total energy, ΔE, and the number ΔN of electrons transferring from M1 to M2, are represented by eqn (7) and (8), as given by Pearson *et al.*:[27,28]

$$\Delta E = -(\chi_{M1} - \chi_{M2})^2/4(\eta_{M1} + \eta_{M2}) \quad (7)$$

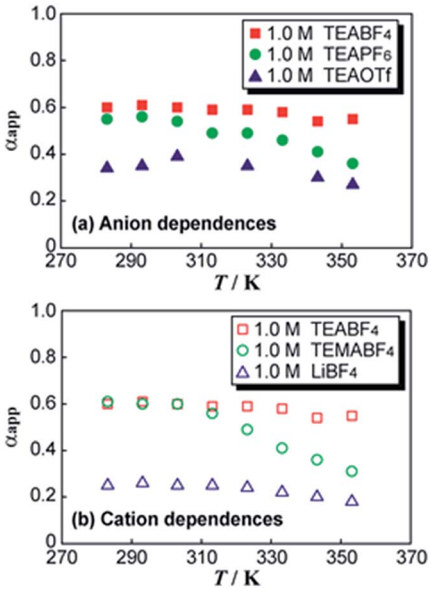

Fig. 9 Plots of degree of dissociation α_{app} for 1.0 M PC electrolytes as a function of temperature for (a) common TEA^+ with three different anions and (b) common BF_4^- with three different cations.

$$\Delta N = (\chi_{M1} - \chi_{M2})/2(\eta_{M1} + \eta_{M2}) \quad (8)$$

where χ and η refer to the absolute electronegativity and absolute hardness of M1 and M2 without interactions, respectively. χ and η are calculated by eqn (9) and (10), respectively:

$$\chi = (I + A)/2 \quad (9)$$

$$\eta = (I - A)/2 \quad (10)$$

where I and A respectively refer to the ionization potential and electron affinity between the interacting species. I and A are calculated by eqn (11) and (12), respectively:

$$I = E(X^{1+}) - E(X^0) \quad (11)$$

$$A = E(X^0) - E(X^{1-}) \quad (12)$$

where $E(X^0)$ refers to the total energy of the interacting species and $E(X^{1-})$ and $E(X^{1+})$ refer to ions having −1 and +1 electrons, respectively. The total energies, $E(X^0)$, $E(X^{1-})$ and $E(X^{1+})$, and the estimated χ and η of the cations and anions are summarized in Table 3. According to the HSAB theory, if χ is higher, the ions and solvent are stronger Lewis acids; if χ is lower, the chemical species is a stronger Lewis base. In addition, a "hard" Lewis acid prefers to interact with a "hard" Lewis base, and a "soft" Lewis acid prefers to interact with a "soft" Lewis base. As shown in Table 3, TEA^+ and $TEMA^+$ exhibited smaller χ values (8.96 and 9.00, respectively) than Li^+ (40.8), indicating that they are weaker Lewis acids.

TEA^+ and $TEMA^+$ therefore weakly interact with anions as Lewis bases, compared with Li^+, as shown in Table 4. In contrast, the hardnesses η of TEA^+ and $TEMA^+$ were smaller (6.42 and 6.46, respectively) than that of Li^+ (35.2), so TEA^+ and $TEMA^+$ prefer to interact with the "soft" Lewis base anion OTf^- (5.00). The orders of magnitude for ΔE and ΔN are $LiBF_4$ > TEAOTf > $TEMABF_4$ ≈ $TEABF_4$ > $TEAPF_6$, which means that $TEAPF_6$ and $TEABF_4$ possess an advantage for the dissociation for their salts.

Considering the solvation energy of ions by PC, ΔE and ΔN for the PC–cation and PC–anion interactions are summarized in Table 5. In general, the ΔE of Li^+–PC is quite large (−7.94 eV), which stabilizes the solvation structure. For the TEA^+ and $TEMA^+$ salts, the PC–cation ΔE is quite small (−0.35 and −0.36 eV, respectively), which is less than 1/20 of that of PC–Li^+.

Table 3 Absolute electronegativity and absolute hardness of cations, anions and PC solvent

Species	$E(X^{1-})$/au	$E(X^0)$/au	$E(X^{1+})$/au	χ/eV	η/eV
TEA^+	−371.620711	−371.527501	−370.962229	8.96	6.42
$TEMA^+$	−332.294914	−332.201415	−331.633078	9.00	6.46
Li^+	−7.49133310	−7.28491780	−4.49025230	40.8	35.2
BF_4^-	−424.480287	−424.679695	−424.410189	0.954	6.38
PF_6^-	−940.707423	−940.896614	−940.597012	1.50	6.65
OTf^-	−961.555515	−961.730421	−961.537879	0.240	5.00
PC	−381.808186	−381.835289	−381.452645	4.84	5.57

Table 4 Interaction energy ΔE and number of electrons transferred ΔN between cations and anions of the salts[a]

Interaction	ΔE/eV	ΔN
$BF_4^- \rightarrow TEA^+$	−1.25	0.313
$PF_6^- \rightarrow TEA^+$	−1.06	0.285
$OTf^- \rightarrow TEA^+$	−1.66	0.382
$BF_4^- \rightarrow TEMA^+$	−1.26	0.314
$BF_4^- \rightarrow Li^+$	−9.56	0.479

[a] ΔE and ΔN correspond to changes in total energy and number of transferred electrons for each interaction, respectively. The arrows show the direction of electron transfer.

Table 5 Interaction energy ΔE and number of electrons transferred ΔN between PC–cation and PC–anion[a]

Interaction	ΔE/eV	ΔN
$PC \rightarrow TEA^+$	−0.354	0.172
$PC \rightarrow TEMA^+$	−0.361	0.173
$PC \rightarrow Li^+$	−7.94	0.441
$PC \rightarrow BF_4^-$	−0.315	0.162
$PC \rightarrow PF_6^-$	−0.227	0.136
$PC \rightarrow OTf^-$	−0.500	0.217

[a] ΔE and ΔN correspond to changes in total energy and number of electrons transferred for each interaction, respectively. The arrows show the direction of electron transfer.

ΔE of the PC–anion interaction was almost same. In addition, ΔE values for the dissociation energies of the salts were also smaller (from −1.06 for $TEABF_4$ to −1.66 eV for TEAOTf) than that of $LiBF_4$ (−9.56 eV). The ammonium salts were, therefore dissociated by interaction between the species. As a result, ammonium cations do not form strong solvation structures as do Li^+-based electrolytes. This leads to electrolytes exhibiting higher μ and n for enhancement of ionic conductively σ: the weak Lewis acidity of TEA^+ and $TEMA^+$ provides the high α_{app} of these salts to increase n in the EDLC electrolytes. Consequently, the $TEABF_4$ salt was most highly dissociated in PC, and the TEA^+ and BF_4^- ions and PC solvent were relatively freely move towards each other in the electrolytes. We therefore have to find an optimum combination of much "softer" and "weaker" Lewis acid cations and much "harder" and "weaker" Lewis base anions to improve the salt dissociation, which will lead to an increase in the number of carrier ions in the capacitor electrolytes. The ionic radii of the cation and anion are also important for capacitor electrolytes because of the relatively weak solvation by PC compared with that in Li^+ electrolytes, such as 1.0 M $LiPF_6$/EC + DEC for LICs[15] and LIBs.[23]

Conclusions

In this study, we discussed ion transport in 1.0 M PC capacitor electrolytes comprising of five salts, *i.e.*, $TEABF_4$, $TEAPF_6$, TEAOTf, $TEMABF_4$ and $LiBF_4$. The mobility of individual ions and PC was determined by self-diffusion coefficients D measured by PGSE-NMR. The $TEABF_4$ electrolyte exhibited the highest D and σ and the lowest η, indicating highest mobility μ of the carrier ions. We also estimated the apparent salt dissociation degree, α_{app} by comparing Λ_{imp} and Λ_{NMR}. The $TEABF_4$ salt exhibited the highest α_{app} among these PC electrolytes in the temperature range from 283 to 353 K. Ion dissociation was shown to have close relations with the Lewis acidity of the cations and Lewis basicity of the anions, under the influence of the hardness and softness of the ions. The target samples of this study are electrolyte systems for electric double layer capacitors, and the salt concentration is relatively low. The experimental findings showed the importance of the quaternary ammonium–BF_4 electrolytes which are currently used in practical EDLC. All the data obtained in this study give sufficient consistency with ionic conductivity. The obtained physical parameters explained the mobility μ and number n of carrier ions in terms of solvation and ion pairs. Control of Lewis acidity and basicity is an important factor to design electrolytes for new-generation electrochemical capacitors. We are undertaking further investigations using new ionic species, such as cyclic cation (spiro-type) salts and low-melting-point salts (ionic liquids), and other solvents, such as acetonitrile towards better systems, based on the concepts in this study.

Acknowledgements

This work was supported by MEXT's scientific technology human resource development grant, "Program to Disseminate Tenure Tracking System," Japan.

References

1 A. D. Pasquier, I. Plitz, S. Menocal and G. G. Amatucci, *J. Power Sources*, 2003, **115**, 171.
2 A. D. Pasquier, I. Plitz, J. Gural, F. Badway and G. G. Amatucci, *J. Power Sources*, 2004, **136**, 160.
3 A. G. Pandolfo and A. F. Hollenkamp, *J. Power Sources*, 2006, **157**, 11.
4 A. Burke, *Electrochim. Acta*, 2007, **53**, 1083.
5 P. Simon and Y. Gogoti, *Nat. Mater.*, 2008, **7**, 845.
6 G. G. Amatucci, F. Badway, A. D. Pasquier and T. Zheng, *J. Electrochem. Soc.*, 2001, **148**, A930.
7 A. D. Pasquier, A. Laforgue, P. Simon, G. G. Amatucci and J.-F. Fauvarque, *J. Electrochem. Soc.*, 2002, **149**, A302.
8 J. R. Dhan and J. A. Seel, *J. Electrochem. Soc.*, 2000, **147**, 899.
9 A. Yoshino, T. Tsubata, M. Shimoyamada, H. Satake, Y. Okano, S. Mori and S. Yata, *J. Electrochem. Soc.*, 2004, **151**, A2180.
10 K. Naoi and P. Simon, *Electrochem. Soc. Interface*, 2008, **17**, 34.
11 K. Naoi, S. Ishimoto, J. Miyamoto and W. Naoi, *Energy Environ. Sci.*, 2012, **5**, 9363.
12 M. Ue, K. Ida and S. Mori, *J. Electrochem. Soc.*, 1994, **141**, 2989.
13 M. Ue, *Electrochemistry*, 2007, **75**(8), 565.
14 K. Chiba, T. Ueda and H. Yamamoto, *Electrochemistry*, 2007, **75**(8), 664.

15 C. Zhong, Y. Deng, W. Hu, J. Qiao, L. Zhang and J. Zhang, *Chem. Soc. Rev.*, 2015, **44**, 7484.
16 M. Ue, *J. Electrochem. Soc.*, 1994, **141**, 3336.
17 R. G. Pearson, *J. Chem. Educ.*, 1968, **45**, 581–643.
18 *Density-Functional Theory of Atoms and Molecules*, ed. R. G. Parr and W. Yang, Oxford University Press, Oxford, UK, 1989.
19 M. Saito, H. Ikuta, Y. Uchimoto and M. Wakihara, *J. Phys. Chem. B*, 2003, **107**, 11608.
20 K. Hayamizu, Y. Aihara, S. Arai and C. G. Martinez, *J. Phys. Chem. B*, 1999, **103**, 519.
21 Y. Aihara, K. Sugimoto, W. S. Price and K. Hayamizu, *J. Chem. Phys.*, 2000, **113**, 1981.
22 K. Hayamizu, E. Akiba, T. Banno and Y. Aihara, *J. Chem. Phys.*, 2002, **117**, 5929.
23 K. Hayamizu, *J. Chem. Eng. Data*, 2012, **57**, 2012.
24 M. J. Frisch, G. W. Trucks, H. B. Schlegel, G. E. Scuseria, M. A. Robb, J. R. Cheeseman, G. Scalmani, V. Barone, B. Mennucci, G. A. Petersson, H. Nakatsuji, M. Caricato, X. Li, H. P. Hratchian, A. F. Izmaylov, J. Bloino, G. Zheng, J. L. Sonnenberg, M. Hada, M. Ehara, K. Toyota, R. Fukuda, J. Hasegawa, M. Ishida, T. Nakajima, Y. Honda, O. Kitao, H. Nakai, T. Vreven, J. A. Montgomery Jr, J. E. Peralta, F. Ogliaro, M. Bearpark, J. J. Heyd, E. Brothers, K. N. Kudin, V. N. Staroverov, R. Kobayashi, J. Normand, K. Raghavachari, A. Rendell, J. C. Burant, S. S. Iyengar, J. Tomasi, M. Cossi, N. Rega, J. M. Millam, M. Klene, J. E. Knox, J. B. Cross, V. Bakken, C. Adamo, J. Jaramillo, R. Gomperts, R. E. Stratmann, O. Yazyev, A. J. Austin, R. Cammi, C. Pomelli, J. W. Ochterski, R. L. Martin, K. Morokuma, V. G. Zakrzewski, G. A. Voth, P. Salvador, J. J. Dannenberg, S. Dapprich, A. D. Daniels, Ö. Farkas, J. B. Foresman, J. V. Ortiz, J. Cioslowski and D. J. Fox, *Gaussian 09, Revision B.01*, Gaussian, Inc., Wallingford CT, 2009.
25 H. Evey, A. G. Bishop, M. Forsyth and D. R. MacFarlane, *Electrochim. Acta*, 2000, **45**, 1279.
26 M. Morita, Y. Asai, N. Yoshimoto and M. Ishikawa, *J. Chem. Soc., Faraday Trans.*, 1998, **94**, 3451.
27 R. G. Parr and R. G. Pearson, *J. Am. Chem. Soc.*, 1983, **105**, 7512.
28 R. G. Pearson, *Inorg. Chem.*, 1984, **23**, 4675.